A Charged Geometric Model for Active Contours

Ronghua Yang and Majid Mirmehdi
Department of Computer Science, University of Bristol, Bristol BS8 1UB, England
{ronghua, majid}@cs.bris.ac.uk

Abstract

This paper presents a new deformable model based on charged particle dynamics and geometric contour propagation. It detects object boundaries with a charged active contour that propagates under the influence of Lorentz forces in an image-based electrostatic field. We make use of level set representation to allow topological changes to be handled naturally. Also, we build on the centre of divergence concept towards automatic initialisation.

1 Introduction

The nonparametric geometric active contour introduced in [1] is a significant improvement over the parametric snake [3] in that it can naturally handle topological changes. However, it still suffers from drawbacks such as a small capture range, edge leakage, and sensitivity to initialisation. There have been numerous improvements and modifications to both parametric and geometric snakes, for example the Gradient Vector Flow (GVF) snake [6] and the geometric GVF snake [4] respectively, which use a bi-directional external force field that provides long-range capture of object boundaries from either side. Nonetheless, these snake models require manual initialisation, especially when there exist internal boundaries separating embedded objects, i.e. an object which has both interior and exterior boundaries.

Recently, a new formulation for a deformable model called the charged particle model (CPM) was introduced by Jalba et al. [2]. CPM can capture object boundaries over the entire image with a set of free charged particles moving in an electrostatic field computed within the image domain. The free charged particles are attracted towards object boundaries by an image-based external force field, while at the same time being repelled by one another by a particle-based internal force. While an initialisation step is still required, it is certainly less pivotal than in the snake model and the charged particles can be placed entirely inside or outside of the object, or across boundaries. This reduced sensitivity to initial conditions is due to CPM's large capture range enabling it to detect boundaries over the entire image. The shortcomings of the CPM model are its weakness in localising objects in busy texture images and that it can not guarantee closed final contours.

Here we propose a novel active contour, the charged contour model (CCM), which defines a geometric active contour based on charged particle dynamics. The motivation is that by combining ideas from the contour and particle models, a more efficient and accurate force field is generated, resulting in a better fitting active contour. CCM is better able in handling highly textured images, and as it is based on geometric contours, it eliminates CPM's possible problem of unclosed contours. It benefits from an image based mesh-to-particle force field as well as geometric contour propagation. However, because it is based on a geometric contour, CCM loses CPM's reduced sensitivity to initialisation. Hence, we also propose an automatic initialisation step which extends the centre of divergence concept in [5].

2 Background

In charged particle dynamics, a set of free-moving positively charged particles is placed in a field that has a distribution of negative fixed charges, forming an electrostatic field around the charged particles. Each particle in the field will then be attracted towards the fixed charges nearby under the influence of a mesh-to-particle (Lorentz) force. Meanwhile, all the positive charges will be repelled by one another by a repulsive particle-to-particle (Coulomb) force.

Consider an electrostatic field with M negative fixed charges and N positive free particles, with the k^{th} fixed charge $e_k < 0$ at grid position $\mathbf{R}_k$, and the i^{th} free particle charge $q_i > 0$ at position $\mathbf{r}_i$. Then, the Lorentz force $\mathbf{F}_l$ (in the absence of a magnetic field) and the Coulomb force $\mathbf{F}_c$ acting on the i^{th} free particle are defined as [2]:

$$\mathbf{F}_l(\mathbf{r}_i) = q_i \sum_{k=1,\mathbf{R}_k \neq \mathbf{r}_i}^{M} \frac{e_k}{4\pi\epsilon_0} \frac{\mathbf{r}_i - \mathbf{R}_k}{|\mathbf{r}_i - \mathbf{R}_k|^3}, \quad (1)$$

$$\mathbf{F}_c(\mathbf{r}_i) = q_i \sum_{j=1,j\neq i}^{N} \frac{q_j}{4\pi\epsilon_0} \frac{\mathbf{r}_i - \mathbf{r}_j}{|\mathbf{r}_i - \mathbf{r}_j|^3}, \quad (2)$$

where ϵ_0 is the electric permittivity of free space. Eq. (1) states that the Lorentz force acting on each free particle is the sum of the forces imposed onto it by all the fixed charges in the electrostatic field. Eq. (2) states that the Coulomb force is the sum of the forces imposed onto a particle by all the other free particles, and as this changes dynamically with distance between particles, it needs to be updated over each particle movement. These two forces play the roles of external and internal forces in a deformable model for image segmentation. The electrostatic field is simulated by equating the edge map magnitude to negative charge e_k for each pixel k.

This CPM model [2] benefits from an initialisation that is largely insensitive to placement without special initial conditions. However, the CPM model is prone to over-segmentation, especially in highly textured images, e.g. see top row of Fig. 6. It can also be seen that CPM can not guarantee closed contours. This inevitably results in breaks and gaps in the recovered object boundaries particularly if the object has weak edges or is partially occluded.

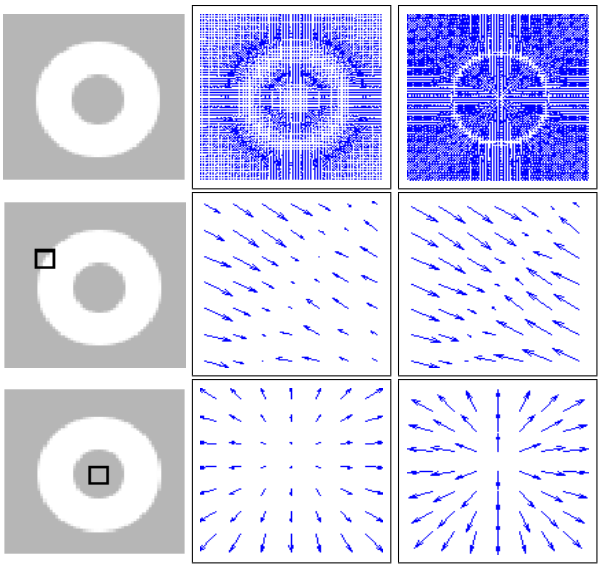

Figure 1. Original and normalised Lorentz fields & close-ups on edge and homogeneous regions.

3 A New Charged Contour Model (CCM)

We propose a model built on the basis of charged particle dynamics and active contour evolution. CCM detects objects starting with a *positively charged active contour* that propagates in an image-based electrostatic field under the influence of Lorentz forces. Since the charged contour is in fact a set of 'connected particles', Coulomb forces do not apply and instead we use the geometric curvature flow for model regulation, implemented using level-sets.

A positively charged contour is placed in an image-based electrostatic field in which each fixed charge is computed as $e_k = -f(x_k, y_k) \leq 0$, where $f(x, y)$ is the image edge map. Then, the Lorentz force field is obtained using (1). As the Lorentz force decays with squared distance, it produces weak flows in homogeneous areas and stronger flows closer to edges. This is an undesirable feature since, driven by these forces, the active contour can hardly move in homogeneous areas, whilst moving fast in edge areas where it is likely to oscillate around edges. As a result, we normalise the Lorentz force field to speed up the model convergence, such that the normalised field has strong flows in homogeneous areas and weak, or close to zero, flows near edges which finally stop the model. At edge locations the strength of the flows are already drastically reduced due to the counteractions among the surrounding fixed charges. This is a good indication of where the real edges are located. Therefore, our edge-preserving normalisation process takes into account the information supplied by the edge map:

$$\mathbf{F}'_l(\mathbf{r}_k) = \frac{\mathbf{F}_l(\mathbf{r}_k)}{|\mathbf{F}_l(\mathbf{r}_k)|} exp(-|e_k|) \qquad (3)$$

where e_k is the fixed charge located at $\mathbf{r}_k$ in the edge map. As $|e_k| \to 0$ in homogeneous areas, then $exp(-|e_k|) \to 1$, and the normalised Lorentz force $\mathbf{F}'_l(\mathbf{r}_k)$ has maximum magnitude tending to unity. When $|e_k|$ increases in edge regions, $exp(-|e_k|)$ scales $\mathbf{F}'_l(\mathbf{r}_k)$ inversely proportional to the edge strength $|e_k|$ and so $\mathbf{F}'_l(\mathbf{r}_k)$ reaches its minimum at the strongest edge location. Thus, the normalised Lorentz force field has the strongest vector flows in homogeneous regions which start to attenuate smoothly when entering edge neighbourhoods. Fig. 1 shows examples of original and normalised Lorentz force field of a simple shape with both interior and exterior boundaries along with a close-up look into both fields. In the homogeneous areas shown, $\mathbf{F}_l$ forces are too weak to propagate the contour model, while the $\mathbf{F}'_l$ forces are sufficiently strong.

We use curvature flow for contour regularisation:

$$\frac{\partial C}{\partial t} = \alpha g(x, y)\kappa \mathbf{N} + (1 - \alpha)(\mathbf{F}'_l \cdot \mathbf{N})\mathbf{N} \qquad (4)$$

where α is a positive constant, κ denotes the curvature flow, $g(x, y) = (1 + f(x, y))^{-1}$ is a stopping term, and $\mathbf{N}$ denotes the contour inward normal. The first term regulates the contour and the second term attracts it towards object boundaries. We embed the charged contour in a level set representation so that it can propagate in the normalised Lorentz force field with topological flexibility:

$$\frac{\partial u}{\partial t} = \alpha g(x, y)\kappa |\nabla u| - (1 - \alpha)\mathbf{F}'_l \cdot \nabla u \qquad (5)$$

where u denotes the level-set. As the geometric contour al-

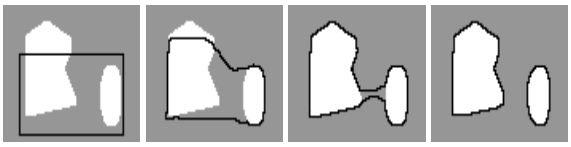

Figure 2. From left: the original image, initial CCM, and snapshots of contour propagation.

ways propagates in the direction of its normal $\mathbf{N}$, it is unable to move when the Lorentz forces are tangent to the contour. We compensate for this by adding an extra adaptive balloon force similar to Paragios et al. [4]. Hence the final formulation of CCM becomes:

$$\frac{\partial C}{\partial t} = \alpha g(x,y)\kappa\mathbf{N} + (1-\alpha)\{(1-\gamma(F_N))F_N + \gamma(F_N)g(x,y)sign(F_N)\}\mathbf{N} \quad (6)$$

where $F_N = \mathbf{F}'_l \cdot \mathbf{N}$ is the component of $\mathbf{F}'_l$ along the contour normal, and $\gamma = exp(-\lambda|.|)$ is a zero-mean Laplacian function which balances the contributions from the Lorentz and extra balloon forces ($\lambda = 3$ in all our experiments determined empirically). When the Lorentz forces and the contour are close to tangent, the balloon force contributes to shrink or expand the contour based on $sign(F_N)$. Otherwise, the contour propagates mainly under the influence of Lorentz forces.

Fig. 2 shows the propagation of CCM on a synthetic image. As can be seen, CCM does not need to be initialised completely exterior or interior to the objects. However, in practice, background noise and features dictate a more elaborate initialisation scheme. Unlike other deformable models based on diffused vector fields, such as the GVF snake [6] and geometric GVF snake [4], the normalised Lorentz field in CCM reflects image features in a more natural manner as it simulates the physical characteristics of image features and does not involve an iterative diffusion process.

4 Automatic Initialisation

In [5], an automatic initialisation approach was demonstrated for the parametric GVF snake in which the directions of every 2×2 neighbouring GVF vectors were examined to determine if they were sufficiently divergent from each other. If so, their position was considered a *centre of divergence* and individual initial contours were automatically placed around them. However, this approach will need to perform at a higher scale (e.g. 3×3) to find centres of divergence in more complex images than those shown in [5]. For example, there are 4 sets of 2×2 neighbouring vectors in the 3×3 centre of divergence shown in Fig. 3(b), and

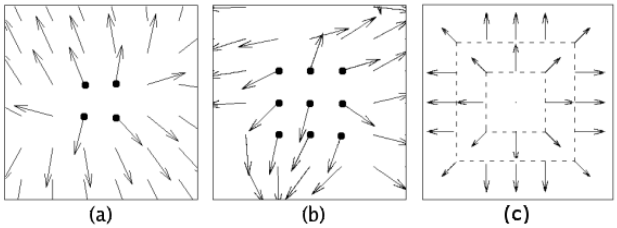

Figure 3. Centre of divergence for (a) a simple shape (b) a real image. (c) outward normal reference vectors for 3x3 and 5x5 windows.

none of them would be considered a centre of divergence by [5] and consequently lead to failure on this detection.

We propose an alternative test for divergence which compares neighbouring vectors with a set of reference vectors and signals a centre of divergence if the vectors' deviation from the reference vectors is within an acceptable range. For a given image, let P_w be the pixels in a window centred at pixel $p(x,y)$ and $\mathbf{N}_w$ be the outward reference vector normals in the window (Fig. 3(c)). We state the potential $\mathcal{P}(x,y)$ of pixel $p(x,y)$ to be a centre of divergence as:

$$\mathcal{P}(x,y) = \sum_w sign[\mathbf{F}'_l(P_w) \cdot \mathbf{N}_w - cos(\frac{\pi}{4})] \quad (7)$$

Each vector around $p(x,y)$ that deviates from its reference vector by $< 45^\circ$ will contribute to the potential of $p(x,y)$ being a centre of divergence. If $\mathcal{P}(x,y)$ is larger than a constant $\mathcal{P}_{min}$ then $p(x,y)$ is considered a centre of divergence. In all our experiments $\mathcal{P}_{min} = 4$. However, if we place an initial contour around every centre of divergence, then contours propagating from both inside and outside the object will merge at object boundaries due to the level-set formulation, and thus lead to false detection. Hence, we select the centres of divergence that are in the brightest regions (top 20%) of the image based on the hypothesis that these will belong either to the object or the background. The contours then segment the object from either the inside or the outside. This works surprisingly well for a variety of images even though initial contours may fall both within and outside the objects of interest (e.g. see middle row of Fig. 5). In comparison, in [5], initial contours are placed around all the centres of divergence, which then necessitates an extra procedure to remove the pseudo boundaries. The number of initial contours does not cost extra in our implementation as they are all handled by the same level set.

Fig. 4 shows an example of our automatic centre of divergence selection. The automatic initialisation scheme proposed here is both convenient for our model and can be used for other vector field based contour models too.

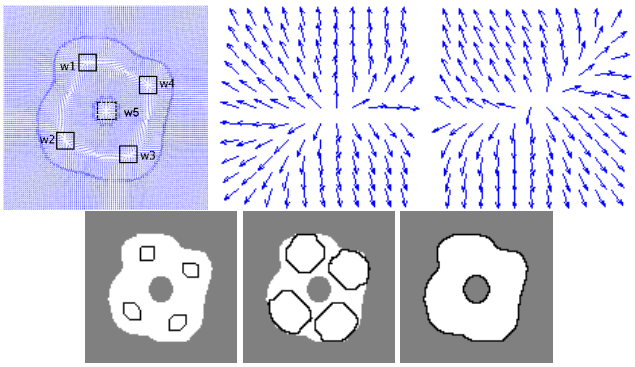

Figure 4. Top: Lorentz force field with centres of divergence (w1-w5). w5 is discarded (outside the object), close-ups of w1 & w3. Bottom: automatic initialisation, propagating CCM, final result.

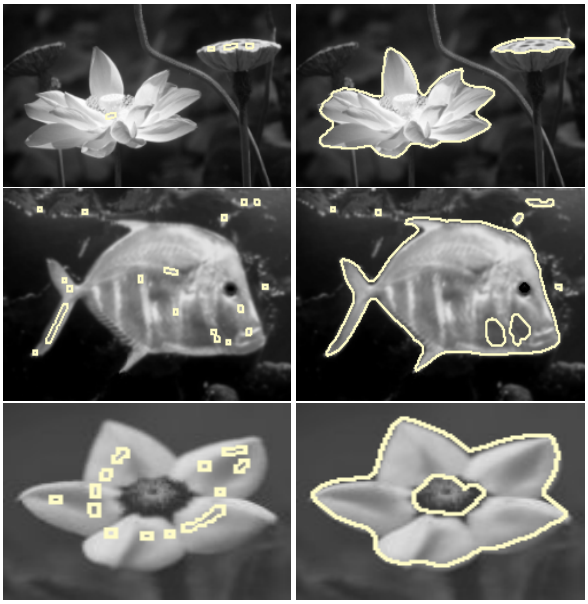

Figure 5. Each row: automatically initialised CCM and final result.

5 Results

CCM has shown promising results and can detect multiple interior and exterior object boundaries (Fig. 5). As mentioned before, CPM [2] can suffer problems on highly textured images, leaving gaps in the recovered boundaries. CCM results in closed boundaries and is more robust to noise as the automatically initialised contours will merge at broken edges or textures that do not belong to any boundaries. Fig. 6 shows a CCM result in comparison to CPM. Further comparative results of CCM against both CPM and geodesic snakes are available online[1].

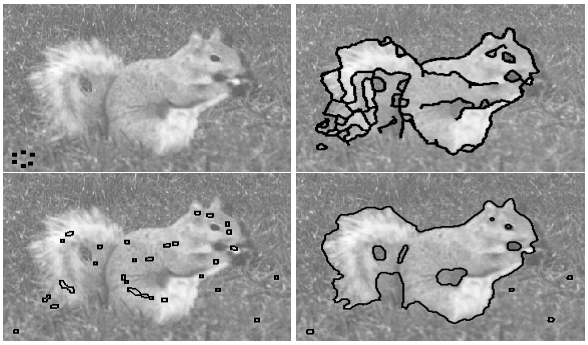

Figure 6. Top: initial CPM particles and final result on a highly textured image. Bottom: automatically initialised and final CCM result.

6 Conclusions

We have introduced a charged contour model for object detection based on charged particle dynamics and active contour propagation. An automatic initialisation approach was also proposed to automate the model. The method is particularly suitable in images where there are one or more specific and salient objects of interest to be found.

A drawback of the current model is that Lorentz forces originating from weak edges may be overcome by those from strong edges nearby, leaving them undetected. Also, the automatic initialisation scheme only works well given that the object and background are different enough so that the centres of divergence either inside or outside the object can be discarded. For future work we plan to extend the particle model to overcome these shortcomings.

References

[1] V. Caselles, R. Kimmel, and G. Sapiro. Geodesic active contours. In *ICCV*, pages 694–699, 1995.

[2] A.C. Jalba, M. Wilkinson, and J. Roerdink. CPM: A deformable model for shape recovery and segmentation based on charged particles. *PAMI*, 26(10):1320–1335, 2004.

[3] P. Kass, A. Witkin, and D. Terzopoulos. Snakes: Active contour models. *IJCV*, 1:321–331, 1988.

[4] N. Paragios, O. Mellina-Gottardo, and V. Ramesh. Gradient vector flow fast geodesic active contours. *PAMI*, 26(3):402–407, 2004.

[5] G. Xingfei and T. Jie. An automatic active contour model for multiple objects. In *ICPR*, pages 881–884, 2002.

[6] C. Xu and J.L. Prince. Gradient vector flow: a new external force for snakes. In *CVPR*, pages 66–71, 1997.

[1] http://vision.cs.bris.ac.uk/AC/CCM/